Selective targeting of $\alpha_4\beta_7$/MAdCAM-1 axis suppresses fibrosis progression in chronic liver disease

Biki Gupta[1]†, **Ravi Prakash Rai**[1]†, Pabitra B. Pal[1], Sudrishti Chaudhary[1], Anna Chiaro[1], Shannon Seaman[1], Aatur D. Singhi[2,3], Satdarshan P. Monga[1,2,4], Smita S. Iyer[1], Reben Raeman*[1,2]

†**Contributed equally**

[1]Division of Experimental Pathology, Department of Pathology, University of Pittsburgh, Pittsburgh, PA. [2]Pittsburgh Liver Research Center, University of Pittsburgh Medical Center and University of Pittsburgh School of Medicine, Pittsburgh, PA USA. [3]Division of Anatomic Pathology, Department of Pathology, University of Pittsburgh School of Medicine, Pittsburgh, PA USA. [4]Division of Gastroenterology, Hepatology and Nutrition, Department of Medicine, University of Pittsburgh School of Medicine, Pittsburgh, PA USA.

***Corresponding Author:**

Reben Raeman, M.S., Ph.D.

Assistant Professor

200 Lothrop Street, S408 BST,

Pittsburgh, PA 15261

Phone: 412-648-2021

Email: reben.raeman@pitt.edu

Keywords: Chronic liver disease; cirrhosis; T cells; fibrosis; inflammation

Conflict of interest: All authors declare no conflicting interests.

Funding: Research reported in this publication was supported by the National Institute of Diabetes and Digestive and Kidney Diseases of the National Institutes of Health under award number K01DK110264 and R01DK124351 to RR; R01DK62277, R01DK100287 and Endowed Chair for Experimental Pathology to SPM; and R56AI150409 and RF1AG06001 to SSI. This research project was also supported in part by the University of Pittsburgh Clinical Biospecimen Processing and Repository Core and Advanced Cell and Tissue imaging Centre of the Pittsburgh Liver Research Centre supported by NIH/NIDDK Digestive Disease Research Core Center grant P30DK120531 and the University of Pittsburgh Unified Flow Core through the resources provided.

Author Contributions. Conceptualization: RR; Methodology: RR, SSI, BG, RPR, PBP, SC, AC, SS, ADS; Investigation: BG, SSI, RPR, PBP; Visualization: RR, BG, RPR, SSI, PBP; Funding acquisition: RR; Project administration: RR, BG, RPR; Supervision: RR; Writing – original draft: BG, RR; Writing – review & editing: RR, SSI, ADS, SPM.

Short Title: $\alpha_4\beta_7$+ T cells promote hepatic fibrosis progression.

ABSTRACT

Integrin $\alpha_4\beta_7$+ T cells perpetuate tissue injury in chronic inflammatory diseases, yet their role in promoting fibrosis in chronic liver diseases (CLD) remains poorly delineated. Here, we examined the role of $\alpha_4\beta_7$+ T cells in promoting fibrosis progression in CLD. Analysis of liver tissue from people with nonalcoholic steatohepatitis (NASH) and alcoholic steatohepatitis (ASH) associated cirrhosis revealed increased accumulation of intrahepatic $\alpha_4\beta_7$+ T cells relative to disease controls. Correspondingly, inflammation and fibrosis in a mouse model of CCl_4-induced liver fibrosis revealed enrichment of intrahepatic $\alpha_4\beta_7$+CD4 and $\alpha_4\beta_7$+CD8 T cells. Monoclonal antibody-mediated blockade of $\alpha_4\beta_7$ or its ligand mucosal addressin cell adhesion molecule (MAdCAM)-1 attenuated hepatic inflammation and fibrosis and prevented disease progression in CCl_4 treated mice. Improvement in liver fibrosis was associated with a significant decrease in hepatic infiltration of $\alpha_4\beta_7$+CD4 and $\alpha_4\beta_7$+CD8 T cells suggesting that $\alpha_4\beta_7$/MAdCAM-1 axis regulates both CD4 and CD8 T cell recruitment to the injured liver and $\alpha_4\beta_7$+CD4 and $\alpha_4\beta_7$+CD8 T cells promote hepatic fibrosis progression. Analysis of $\alpha_4\beta_7$+ and $\alpha_4\beta_7$- CD4 T cells revealed that $\alpha_4\beta_7$+ CD4 T cells enriched for markers of activation and proliferation demonstrating an effector phenotype. The findings suggest that $\alpha_4\beta_7$/MAdCAM-1 axis play a critical role in promoting fibrosis progression in CLD by recruiting CD4 and CD8 T cells to the liver, and mAb-mediated blockade of $\alpha_4\beta_7$ or MAdCAM-1 represents a novel therapeutic strategy to slow CLD progression.

INTRODUCTION

Wound healing and repair are fundamental biological processes critical to maintaining tissue architecture and restoring organ homeostasis following injury (1). Protracted injury, however, can dysregulate this process resulting instead in excessive extracellular matrix deposition and tissue scarring or fibrosis. Progressive fibrosis is characteristic of advanced chronic liver diseases (CLDs), including alcoholic and nonalcoholic steatohepatitis as well as viral and autoimmune hepatitis(2-4). Chronic unresolved fibrosis can lead to cirrhosis, the 11th leading cause of global deaths, and a major risk factor for developing hepatocellular carcinoma (HCC) which is among the top 20 causes of deaths worldwide. Consequently, therapeutic strategies to stop progression of fibrosis in CLD are urgently needed.

The inflammatory response to liver injury, essential for resolution of injury and tissue repair, is a highly regulated process where both the initiation and resolution of inflammation are mediated by the liver-resident and liver-recruited immune cells. Chronic injury, however, leads to a perpetuation of hepatic inflammation characterized by sustained infiltration of immune cells to the liver and maintenance of fibrogenic pathways. While the liver-resident macrophages or Kupffer cells (KC) play a key role in the initiation of inflammation, recent data show that they are depleted in the advanced stages of CLD. Ultimately, the recruited proinflammatory immune cells including cells of both myeloid and lymphoid origin play a more prominent role in fibrosis progression making them an interesting target for therapeutic approaches to address CLD (5).

Immune cell recruitment to the liver following injury is mediated by chemokines and cytokines released by damaged hepatocytes, activated KCs as well as HSC-derived myofibroblasts.

Recently, we demonstrated that the heterodimeric integrin receptor $\alpha_4\beta_7$ expressed on immune cells and its ligand, mucosal addressin cell adhesion molecule (MAdCAM)-1, expressed on endothelial cells, drive hepatic inflammation in NASH by promoting recruitment of $\alpha_4\beta_7$+ CD4 T cells to the liver (6). The $\alpha_4\beta_7$/MAdCAM-1 axis is also implicated in promoting hepatic inflammation in chronic inflammatory liver diseases and primary sclerosing cholangitis (PSC), and upregulation of MAdCAM-1 expression is reported in cirrhotic livers (7-9). Despite strong evidence suggesting that the $\alpha_4\beta_7$/MAdCAM-1 axis is influential in CLD, role of $\alpha_4\beta_7$/MAdCAM-1 axis in promoting hepatic fibrosis progression remain poorly delineated.

In the current study we show a critical role of $\alpha_4\beta_7$/MAdCAM-1 axis in promoting fibrosis progression in CLD. We demonstrate that people with NASH and ASH-associated cirrhosis have higher accumulation of $\alpha_4\beta_7$+ T cells in the liver relative to disease controls. Enrichment of $\alpha_4\beta_7$+CD4 and $\alpha_4\beta_7$+CD8 T cells was also observed in a mouse model of liver fibrosis. Therapeutic blockade of $\alpha_4\beta_7$ or MAdCAM-1 in a mouse model of fibrosis attenuated hepatic inflammation and fibrosis progression. Improvement in liver fibrosis was associated with a significant decrease in the recruitment of $\alpha_4\beta_7$+CD4 and $\alpha_4\beta_7$+CD8 T cells as well as monocytes and macrophages in the liver. Together our findings indicate that $\alpha_4\beta_7$+CD4 and $\alpha_4\beta_7$+CD8 T cells promote fibrosis progression in CLD and blocking $\alpha_4\beta_7$/MAdCAM-1-mediated recruitment of $\alpha_4\beta_7$+ T cells to the liver may represent a novel therapeutic strategy to slow or prevent fibrosis progression in CLD.

METHODS

Mice. Adult male C57BL/6J mice were obtained from The Jackson Laboratory (Bar Harbor, ME). The mice were maintained at the University of Pittsburgh Division of Animal Resources. Age- and sex-matched littermates were used for all experiments at 8–10 wk of age. All animal studies were carried out in accordance with protocols approved by the Institutional Animal Care and Use Committee at the University of Pittsburgh.

Human tissue. De-identified, fixed explanted liver tissues from people receiving orthotopic liver transplantation for decompensated liver cirrhosis were obtained from Biospecimen Processing and Repository Core at Pittsburgh Liver Research Centre.

Integrin $\alpha_4\beta_7$ and MAdCAM-1 antibody treatment. To induce hepatic fibrosis, eight-week-old male mice were given twice weekly oral gavage of CCl_4 (in 1:1 v/v olive oil) for six weeks. Mice receiving equal volume of olive oil served as controls. After 2 weeks of CCl_4 treatment, a cohort of mice were treated with twice weekly intraperitoneal injections of 8 mg/Kg $\alpha_4\beta_7$ mAb (DATK32; Bioxcell, West Lebanon, NH) or MAdCAM-1 mAb (MECA-367; Bioxcell, West Lebanon, NH) or rat IgG2a isotype antibody (Bioxcell, West Lebanon, NH) for four weeks.

Histopathology. Histopathological analyses, including Hematoxylin and eosin (H&E) and Sirius Red staining, were conducted on formalin-fixed liver tissue sections as previously reported.(10) Photomicrographs of the histologic sections were obtained by using a Zeiss Light Microscope (Zeiss, Jena, Germany).

Immunofluorescence microscopy. Immunofluorescence (IF) microscopy was conducted on liver cryosections as previously reported.(10) The IF images were visualized and obtained by using an Axioskop 2 plus microscope (Zeiss, Jena, Germany). Following antibodies were used for mouse tissue, $\alpha_4\beta_7$/LPAM1(cat. No. 120702, Clone: MECA-367, Biolegend), aSMA (cat. No. MA1-06110, ThermoFisher Scientific), MAdCAM1(cat. No. 16-5997-85, ThermoFisher Scientific). Following antibodies were used for human tissue, $\alpha_4\beta_7$/LPAM1(cat. No. DDX1434P-100, Clone: 11D9.03, Novus Biologicals) and CD3 (cat. No. ab135372, Abcam),

Serological analysis. Serum alanine aminotransferase (ALT), and aspartate aminotransferase (AST) concentrations were measured using an AST and ALT Activity Assay Kit (Sigma-Aldrich, St. Louis, MO).

Flow cytometric analysis. Livers perfused with 1X PBS (Thermo Fisher Scientific, Waltham, MA) were digested with 2mg/mL type IV collagenase (Worthington, NY) to obtain single cell suspensions and the lymphocytes were enriched by Percoll gradient centrifugation as describes previously (10). Enriched lymphocytes were stained with fluorochrome-conjugated antibodies and fixable viability stain (BD Biosciences, San Jose, CA), and samples were acquired on Cytek Aurora Spectral Cytometer (Cytek Biosciences, Bethesda, MD) equipped with five lasers. Data were analyzed using FlowJo software v X.10 (Tree Star, Inc., Ashland, OR). Fuorochrome conjugated antibodies against CD45 (30-F11), CD3 (17A2), CD4 (RM4-5), CD8 (53-6.7), CD44 (IM7), CD69 (H1.2F3), Tbet (4B10) and $\alpha_4\beta_7$ (LPAM-1; DATK32) were purchased from BD Biosciences (San Jose, CA), and Foxp3 (FJK-16s), Ki67 (SolA15) and Live/Dead Aqua was purchased form ThermoFisher Scientific (Waltham, MA).

Quantitative real-time PCR. Isolation of total RNA from liver, cDNA synthesis and qRT-PCR were performed as previously described.(10) Data were normalized to 18S rRNA and data are presented as fold change in gene expression compared to controls.

Statistical analysis. Two-tailed Student's t test was employed to compare mean differences between two groups. One-way ANOVA in conjunction with post-hoc analysis for multiple group comparison was employed to investigate statistical differences. A p value < 0.05 was considered statistically significant. Data shown are representative of 3 independent experiments. Statistical analyses were performed using GraphPad Prism 8.0 (GraphPad Software) software.

RESULTS

Increased infiltration of $\alpha_4\beta_7$+ T cells in the livers of NASH- and ASH-associated cirrhosis patients.

We recently demonstrated that blocking $\alpha_4\beta_7$+ T cell recruitment to the liver reduces hepatic injury in a murine model of NASH (6). To determine whether $\alpha_4\beta_7$+ T cells are also involved in the hepatic inflammation and fibrosis in people with end-stage liver disease, we probed liver tissue sections obtained from 10 people with NASH-associated cirrhosis and 10 people with ASH-associated cirrhosis for the presence of $\alpha_4\beta_7$+ T cells using confocal laser scanning microscopy. Liver tissue from tumor-adjacent parenchyma was used as controls. People with NASH- and ASH-associated cirrhosis had high serum transaminases, bilirubin and GGT levels and extensive fibrotic septa in the liver (**Fig. 1A-1E**). Liver tissue sections stained with $\alpha_4\beta_7$ and CD3 antibodies revealed higher infiltration of $\alpha_4\beta_7$ and CD3 double-positive T cells and

formation of large inflammatory aggregates of $\alpha_4\beta_7$+ T cells in the livers of people with NASH- and ASH-associated cirrhosis (**Fig. 1F**). Interestingly, higher inflammatory aggregates of $\alpha_4\beta_7$+CD3+ T cells were observed in the fibrotic septa in the livers of people with NASH-associated cirrhosis when compared to people with ASH-associated cirrhosis. Collectively, these findings suggest the involvement of $\alpha_4\beta_7$+ T cells in people with end-stage liver disease.

Integrin $\alpha_4\beta_7$ blockade attenuates CCl_4-induced hepatic inflammation.

Given the increased hepatic infiltration of $\alpha_4\beta_7$+ T cells in people with cirrhosis, we used a mouse model of liver fibrosis to investigate whether blocking recruitment of $\alpha_4\beta_7$+ T cells would be effective in decreasing hepatic inflammation and fibrosis progression. Liver fibrosis was induced by oral administration of CCl_4 for six weeks. Mice administered the vehicle, olive oil, served as controls. A cohort of CCl_4-treated mice received $\alpha_4\beta_7$ mAb for four weeks starting at week three. Mice treated with IgG isotype antibody served as controls (CCl_4 + IgG) (**Fig. 2A**). As shown in **Fig. 2B**, CCl_4 + IgG-treated mice experienced severe liver injury indicated by increased infiltration of immune cells, steatosis and necrotic hepatocytes corroborated by high serum aspartate aminotransferase (AST) and alanine aminotransferase (ALT) levels relative to vehicle controls (**Fig. 2C-D**). Transcript levels of key pro-inflammatory cytokines, tumor necrosis factor-α (TNFα) and interleukin, IL-6, were also significantly upregulated in the livers of CCl_4 + IgG- treated mice relative to controls indicative of severe hepatic inflammation (**Fig. 2E-F**). In contrast, histological analysis of liver tissue sections from CCl_4 + $\alpha_4\beta_7$-mAb-treated mice revealed substantial improvement in hepatic inflammation as evidenced by reduced infiltration of immune cells and reduced tissue injury (**Fig. 2B**). The marked attenuation of liver injury in CCl_4 + $\alpha_4\beta_7$-mAb treated mice was further substantiated by significantly reduced serum

ALT and AST levels (**Fig. 2C-D**). Compared to IgG controls, $\alpha_4\beta_7$ mAb treatment also significantly reduced transcript levels of key pro-inflammatory cytokines, TNF-α and IL-6 in the liver (**Fig. 2E-F**). Collectively, these results demonstrate that $\alpha_4\beta_7$ blockade protected mice from CCl_4-induced hepatic inflammation and injury.

Integrin $\alpha_4\beta_7$ blockade reduces hepatic fibrosis progression.

To determine the effect of $\alpha_4\beta_7$ blockade on hepatic fibrosis, liver tissue sections were stained with Sirius Red to assess collagen deposition while transcript levels of key molecules associated with hepatic fibrogenesis were quantified by qRT-PCR. As shown in **Fig. 3A**, CCl_4 treatment induced severe hepatic fibrosis indicated by increased collagen deposition in the livers of CCl_4 + IgG-treated mice relative to vehicle controls. The transcript levels of fibrogenesis marker α-smooth muscle actin (αSMA), a key marker of hepatic stellate cell (HSC) activation, collagen I (Col IAI and Col IAII), transforming growth factor-β1 (TGF-β1), and tissue inhibitor of metalloproteinase-1 (TIMP-1) were also significantly elevated in the CCl_4 + IgG-treated mice relative to controls (**Fig. 3B-F**). Treatment with $\alpha_4\beta_7$ mAb reduced hepatic fibrosis reflected by decreased collagen deposition in the liver and significant reduction in the transcript levels of αSMA, Col IAI and Col IAII, TGF-β1 and TIMP-1 (**Fig. 3A-F**). These results were further corroborated by confocal imaging of αSMA-stained liver tissue sections demonstrating significant inhibition of HSC activation evidenced by reduced hepatic αSMA-expressing HSCs following $\alpha_4\beta_7$ mAb treatment (**Fig. 3G**). Taken together, these results demonstrate that $\alpha_4\beta_7$ blockade attenuates CCl_4-induced hepatic fibrosis.

$\alpha_4\beta_7$ mAb treatment reduces CCl_4-induced infiltration of $\alpha_4\beta_7$+ T cells in the liver.

To determine whether $\alpha_4\beta_7$ mAb treatment reduced hepatic inflammation and fibrosis in CCl_4-treated mice by reducing recruitment of $\alpha_4\beta_7$+ immune cells to the liver, we first assessed hepatic expression of $\alpha_4\beta_7$ using confocal laser scanning microscopy. As shown in **Fig 4A**, $\alpha_4\beta_7$+ cell infiltration was higher in the livers of CCl_4 + IgG-treated mice relative to controls. Increased $\alpha_4\beta_7$+ cells in the fibrotic liver was further corroborated by increased expression of integrins α_4 and β_7 transcripts in the liver of CCl_4 + IgG-treated mice relative to vehicle controls (**Fig. 4B-D**). Treatment with $\alpha_4\beta_7$ mAb decreased $\alpha_4\beta_7$+ cell infiltration indicated by decreased $\alpha_4\beta_7$+ cells in the liver sections of CCl_4 + $\alpha_4\beta_7$ mAb-treated mice relative to IgG-treated mice (**Fig 4A)**. When compared to CCl_4 + IgG-treated mice, $\alpha_4\beta_7$ mAb treatment reduced inflammatory aggregates formed by $\alpha_4\beta_7$+ cells. Treatment with $\alpha_4\beta_7$ mAb also significantly reduced transcript levels of integrins α_4 and β_7, but not β_1 demonstrating that $\alpha_4\beta_7$ blockade reduces the increase in $\alpha_4\beta_7$+ cell infiltration in the liver caused by CCl_4 (**Fig. 4A-D**).

Having established increased infiltration of $\alpha_4\beta_7$+ cells in the fibrotic liver and a marked decrease in $\alpha_4\beta_7$+ cells in the CCl_4 + $\alpha_4\beta_7$ mAb-treated mice, we sought to delineate hepatic immune cell subsets by flow cytometry. Analysis of intrahepatic lymphocytes revealed significant increases in the frequency and the total numbers of CD4 (CD3+CD4+) and CD8 (CD3+CD8+) T cells in the livers of the CCl_4 + IgG-treated mice relative to vehicle controls (**Fig. 4E-F, Sup. Fig. 1A**). Further analysis revealed increased frequency and total numbers of intrahepatic CD4 and CD8 T cells expressing $\alpha_4\beta_7$ in the CCl_4 + IgG-treated mice suggesting increased recruitment of $\alpha_4\beta_7$+ T cells to the liver (**Fig. 4G-H**). The treatment with $\alpha_4\beta_7$ mAb significantly reduced the frequency and total numbers of $\alpha_4\beta_7$+ CD4 and CD8 T cells in the liver of CCl_4-treated mice compared to IgG controls as well as total CD4 and CD8 T numbers but not frequencies (**Fig. 4E-H and Sup.**

Fig. 1A). The treatment with $\alpha_4\beta_7$ mAb also significantly reduced CD44+$\alpha_4\beta_7$+ CD4 T cells but did not affect the frequency and the total numbers of Foxp3+ T regulatory cells in the liver (**Sup. Fig. 1B-E**). Together, these findings indicate a pivotal role for $\alpha_4\beta_7$+ T cells in promoting hepatic inflammation and fibrosis in CCl_4-treated mice.

MAdCAM-1 blockade reduces CCl_4-induced hepatic infiltration of $\alpha_4\beta_7^+$ T cells

To determine if MAdCAM-1 blockade would similarly impact hepatic T cell recruitment in CCl_4-treated mice and ultimately attenuate liver injury, a cohort of the CCl_4-treated mice received MAdCAM-1 mAb for four weeks. Mice treated with IgG isotype served as controls. As seen in **Fig. 5A-D**, four weeks of treatment with MAdCAM-1 mAb resulted in a decrease in the frequency and the total number of $\alpha_4\beta_7$+CD4 and $\alpha_4\beta_7$+CD8 T cells in the livers of CCl_4 + MAdCAM-1 mAb-treated mice relative to IgG treatment. No changes in the frequencies and the total number of intrahepatic CD4 and CD8 T cells as well as T regulatory cells were observed in the MAdCAM-1 mAb treated mice compared to IgG controls (**Supp. Fig. 2A-E**). MAdCAM-1 mAb treatment also decreased the frequency and the total numbers of macrophages (CD3-CD11b+Ly6G-F4/80+ cells) and monocytes (CD3-CD11b+Ly6G-Ly6C+ cells) in the livers of CCl_4-treated mice relative to IgG treatment (**Fig. 5E-F**). Furthermore, transcript levels of integrins α_4 and β_7 and MAdCAM-1 were also significantly lower in the CCl_4 + MAdCAM-1 mAb-treated mice (**Fig. 5G-I**). These data demonstrate that MAdCAM-1 blockade also reduces recruitment of $\alpha_4\beta_7$+ T cells to the injured liver.

$\alpha_4\beta_7$+ CD4 T cells enriched for markers of activation and proliferation demonstrating an effector phenotype.

To determine the function of $\alpha_4\beta_7$ we assessed $\alpha_4\beta_7$ + and $\alpha_4\beta_7$ - CD4 T subsets in the liver of CCl_4 + IgG treated mice for expression of T cell activation and proliferation markers. Our analysis revealed that a significantly higher frequency of $\alpha_4\beta_7$+ CD4 T cells expressed T cell activation markers CD44 and the acute activation surface receptor, CD69, Th1 transcriptional factor driving IFN production Tbet and the cell proliferation marker Ki67 compared to the $\alpha_4\beta_7$- CD4 T cells (**Fig 6A-D**). These data suggest that $\alpha_4\beta_7$+ CD4 T cells comprise effector T cells with capacity for proliferation and cytokine production.

MAdCAM-1 blockade attenuates CCl_4-induced hepatic injury and fibrosis.

Given the inhibitory effect of MAdCAM-1 blockade on the CCl_4-induced recruitment of immune cells to the liver, we examined whether MAdCAM-1 blockade also reduced CCl_4-induced liver injury. Histological analysis of H&E-stained liver tissue sections revealed a notable decrease in hepatic inflammation and injury in CCl_4 + MAdCAM-1-mAb treated mice compared to the CCl_4 + IgG-treated mice (**Fig. 7A**). Improvement in hepatic inflammation and injury in CCl_4 + MAdCAM-1-mAb treated mice was confirmed by decreased serum ALT levels (**Fig. 7B**) as well as significant down-regulation in the transcript levels of TGF-β and IL6, but not TNF-α (**Fig. 7C-E**). MAdCAM-1 mAb treatment also decreased hepatic fibrosis indicated by marked decrease in the deposition of hepatic collagen in the Sirius Red-stained liver tissue sections (**Fig. 7F**). Transcript levels of key molecules associated with fibrogenesis of the liver, αSMA, TIMP-1, and Col IAI and Col IAII were significantly lower in the MAdCAM-1-mAb-treated mice relative to IgG controls (**Fig. 7G-J**). These data further underscore the importance of the $\alpha_4\beta_7$/MAdCAM-1 axis in promoting CCl_4-induced liver inflammation and fibrosis.

DISCUSSION

Immune cells recruited to the injured liver are the primary instigators of sustained chronic inflammation and resulting fibrosis in CLD[11-14]; yet we lack complete understanding of the molecular mechanisms involved in immune-cell recruitment and the role of various immune cells in promoting fibrosis progression in CLD. Here, we report a pivotal role of $\alpha_4\beta_7$/MAdCAM-1 axis in recruiting $\alpha_4\beta_7$+CD4 and $\alpha_4\beta_7$+CD8 T cells to the injured liver and a critical role of $\alpha_4\beta_7$+CD4 and $\alpha_4\beta_7$+CD8 T cells in promoting hepatic fibrosis progression in CLD.

Our clinical data demonstrating inflammatory aggregates of $\alpha_4\beta_7$+ T cells in the livers of people with cirrhosis provide a clear and distinct indication that $\alpha_4\beta_7$+ T cells is important in promoting liver injury in cirrhosis. Interestingly, $\alpha_4\beta_7$+ T cells form larger inflammatory aggregates in the livers of people with NASH-associated cirrhosis compared to those with ASH-associated cirrhosis suggesting a more prominent role of $\alpha_4\beta_7$+ T cells in contributing to liver injury in NASH-associated cirrhosis. The presence of $\alpha_4\beta_7$+ T cells in the livers of people without known liver disease strongly suggest $\alpha_4\beta_7$+ T cells are also instrumental in liver homeostasis. Further investigation is needed to determine whether $\alpha_4\beta_7$+ T cells are actively recruited to the normal liver or whether $\alpha_4\beta_7$ is imprinted on hepatic T cells and their contribution to liver homeostasis.

Our findings from the mouse model of CCl_4-induced liver fibrosis recapitulated clinical findings by revealing enrichment of $\alpha_4\beta_7$+ T cells and elevated MAdCAM-1 expression in the fibrotic liver. Supporting a mechanistic role of $\alpha_4\beta_7$+ T cells in promoting hepatic inflammation and fibrosis, mAb-mediated blockade of $\alpha_4\beta_7$ or MAdCAM-1-reversed CCl_4-induced hepatic inflammation and fibrosis progression. These findings together with previous reports of the

involvement of the $\alpha_4\beta_7$/MAdCAM-1 axis in regulating immune-cell recruitment to the livers of people with NASH, PSC and other immune and infectious diseases of the liver suggest a critical role of the $\alpha_4\beta_7$/MAdCAM-1 axis in promoting hepatic inflammation and fibrosis progression in CLD (8, 15, 16).

The role of innate immune cells in promoting liver fibrosis is well defined, but our understanding of the mechanisms regulating adaptive immune cell recruitment to the liver and their role in driving fibrosis progression remains less well-defined. In the context of tissue injury and fibrosis, the role of CD8 T cells is of special interest as antigen-specific or bystander activation of CD8 T cells can promote tissue injury by cytolysis of damaged cells or exacerbate inflammation by producing proinflammatory cytokines including TNF-α, INF-γ, (17, 18), IL-13(19, 20) and IL-4 (21), which amplifies recruitment of proinflammatory immune cells to the injured tissue. Our data provide evidence for a role of $\alpha_4\beta_7$/MAdCAM-1 axis in regulating hepatic CD8 T cell recruitment by demonstrating that a significant subset of CD8 T cells express $\alpha_4\beta_7$, and $\alpha_4\beta_7$ and MAdCAM-1-blocking antibodies reduce recruitment of $\alpha_4\beta_7$+CD8 T cells to the livers of CCl_4-treated mice. This finding is an important addition to the previously reported roles of the $\alpha_4\beta_7$/MAdCAM-1 axis in CD4 T cell homing to the liver in NASH(6) and PSC (16). Our data demonstrating that blockade of $\alpha_4\beta_7$+CD8 T cell recruitment to the liver improves hepatic injury in CCL_4-treated mice as well as previous studies reporting that $\alpha_4\beta_7$ is a marker of effector T cells (22, 23) suggest that $\alpha_4\beta_7$-expressing CD8 T cells may play a prominent role in promoting liver injury in CLD. However, considering reports that CD8 T cells play a protective role during hepatic injury resolution by eliminating activated HSCs (24), and their dysfunction at the advanced stages of CLD exacerbate disease progression (25, 26), further in-depth studies are

necessary to determine the function of CD8 T cell subsets in promoting inflammation as well as resolution of injury in CLD.

Our results provide a deeper understanding of the impact of the $\alpha_4\beta_7$/MAdCAM-1 axis in immune-mediated regulation of inflammation and fibrosis in liver injury, and proffer mAb-mediated blockade of integrin $\alpha_4\beta_7$ or MAdCAM-1 as an approach in the treatment of inflammation and fibrosis in chronic liver diseases.

REFERENCES

1. Koyama, Y., and Brenner, D. A. (2017) Liver inflammation and fibrosis. *J Clin Invest* **127**, 55-64
2. Lackner, C., and Tiniakos, D. (2019) Fibrosis and alcohol-related liver disease. *J Hepatol* **70**, 294-304
3. Alkhouri, N., and McCullough, A. J. (2012) Noninvasive Diagnosis of NASH and Liver Fibrosis Within the Spectrum of NAFLD. *Gastroenterol Hepatol (N Y)* **8**, 661-668
4. Pinzani, M., Rombouts, K., and Colagrande, S. (2005) Fibrosis in chronic liver diseases: diagnosis and management. *J Hepatol* **42 Suppl**, S22-36
5. Wen, Y., Lambrecht, J., Ju, C., and Tacke, F. (2021) Hepatic macrophages in liver homeostasis and diseases-diversity, plasticity and therapeutic opportunities. *Cell Mol Immunol* **18**, 45-56
6. Rai, R. P., Liu, Y., Iyer, S. S., Liu, S., Gupta, B., Desai, C., Kumar, P., Smith, T., Singhi, A. D., Nusrat, A., Parkos, C. A., Monga, S. P., Czaja, M. J., Anania, F. A., and Raeman, R. (2020) Blocking integrin alpha4beta7-mediated CD4 T cell recruitment to the intestine and liver protects mice from western diet-induced non-alcoholic steatohepatitis. *J Hepatol*
7. Ala, A., Brown, D., Khan, K., Standish, R., Odin, J. A., Fiel, M. I., Schiano, T. D., Hillan, K. J., Rahman, S. A., Hodgson, H. J., and Dhillon, A. P. (2013) Mucosal addressin cell adhesion molecule (MAdCAM-1) expression is upregulated in the cirrhotic liver and immunolocalises to the peribiliary plexus and lymphoid aggregates. *Dig Dis Sci* **58**, 2528-2541

8. Grant, A. J., Lalor, P. F., Hubscher, S. G., Briskin, M., and Adams, D. H. (2001) MAdCAM-1 expressed in chronic inflammatory liver disease supports mucosal lymphocyte adhesion to hepatic endothelium (MAdCAM-1 in chronic inflammatory liver disease). *Hepatology* **33**, 1065-1072

9. Borchers, A. T., Shimoda, S., Bowlus, C., Keen, C. L., and Gershwin, M. E. (2009) Lymphocyte recruitment and homing to the liver in primary biliary cirrhosis and primary sclerosing cholangitis. *Semin Immunopathol* **31**, 309-322

10. Rahman, K., Desai, C., Iyer, S. S., Thorn, N. E., Kumar, P., Liu, Y., Smith, T., Neish, A. S., Li, H., Tan, S., Wu, P., Liu, X., Yu, Y., Farris, A. B., Nusrat, A., Parkos, C. A., and Anania, F. A. (2016) Loss of Junctional Adhesion Molecule A Promotes Severe Steatohepatitis in Mice on a Diet High in Saturated Fat, Fructose, and Cholesterol. *Gastroenterology* **151**, 733-746 e712

11. Karlmark, K. R., Wasmuth, H. E., Trautwein, C., and Tacke, F. (2008) Chemokine-directed immune cell infiltration in acute and chronic liver disease. *Expert Rev Gastroenterol Hepatol* **2**, 233-242

12. Karlmark, K. R., Weiskirchen, R., Zimmermann, H. W., Gassler, N., Ginhoux, F., Weber, C., Merad, M., Luedde, T., Trautwein, C., and Tacke, F. (2009) Hepatic recruitment of the inflammatory Gr1+ monocyte subset upon liver injury promotes hepatic fibrosis. *Hepatology* **50**, 261-274

13. Pellicoro, A., Ramachandran, P., Iredale, J. P., and Fallowfield, J. A. (2014) Liver fibrosis and repair: immune regulation of wound healing in a solid organ. *Nat Rev Immunol* **14**, 181-194

14. Kisseleva, T., and Brenner, D. (2021) Molecular and cellular mechanisms of liver fibrosis and its regression. *Nat Rev Gastroenterol Hepatol* **18**, 151-166

15. Hillan, K. J., Hagler, K. E., MacSween, R. N., Ryan, A. M., Renz, M. E., Chiu, H. H., Ferrier, R. K., Bird, G. L., Dhillon, A. P., Ferrell, L. D., and Fong, S. (1999) Expression of the mucosal vascular addressin, MAdCAM-1, in inflammatory liver disease. *Liver* **19**, 509-518

16. de Krijger, M., Wildenberg, M. E., de Jonge, W. J., and Ponsioen, C. Y. (2019) Return to sender: Lymphocyte trafficking mechanisms as contributors to primary sclerosing cholangitis. *J Hepatol* **71**, 603-615

17. Neurath, M. F. (2014) Cytokines in inflammatory bowel disease. *Nat Rev Immunol* **14**, 329-342

18. Kopf, M., Bachmann, M. F., and Marsland, B. J. (2010) Averting inflammation by targeting the cytokine environment. *Nat Rev Drug Discov* **9**, 703-718

19. Fuschiotti, P., Larregina, A. T., Ho, J., Feghali-Bostwick, C., and Medsger, T. A., Jr. (2013) Interleukin-13-producing CD8+ T cells mediate dermal fibrosis in patients with systemic sclerosis. *Arthritis Rheum* **65**, 236-246

20. Fuschiotti, P. (2018) Current perspectives on the role of CD8+ T cells in systemic sclerosis. *Immunol Lett* **195**, 55-60

21. Nakamura, K., Amakawa, R., Takebayashi, M., Son, Y., Miyaji, M., Tajima, K., Nakai, K., Ito, T., Matsumoto, N., Zen, K., Kishimoto, Y., and Fukuhara, S. (2005) IL-4-producing CD8(+) T cells may be an immunological hallmark of chronic GVHD. *Bone Marrow Transplant* **36**, 639-647

22. Wittner, M., Schlicker, V., Libera, J., Bockmann, J. H., Horvatits, T., Seiz, O., Kummer, S., Manthey, C. F., Hufner, A., Kantowski, M., Rosch, T., Degen, O., Huber, S., Eberhard, J. M., and Schulze Zur Wiesch, J. (2019) Comparison of the integrin alpha4beta7 expression pattern of memory T cell subsets in HIV infection and ulcerative colitis. *PLoS One* **14**, e0220008

23. Kurmaeva, E., Lord, J. D., Zhang, S., Bao, J. R., Kevil, C. G., Grisham, M. B., and Ostanin, D. V. (2014) T cell-associated α4β7 but not α4β1 integrin is required for the induction and perpetuation of chronic colitis. *Mucosal Immunol* **7**, 1354-1365

24. Koda, Y., Teratani, T., Chu, P. S., Hagihara, Y., Mikami, Y., Harada, Y., Tsujikawa, H., Miyamoto, K., Suzuki, T., Taniki, N., Sujino, T., Sakamoto, M., Kanai, T., and Nakamoto, N. (2021) CD8(+) tissue-resident memory T cells promote liver fibrosis resolution by inducing apoptosis of hepatic stellate cells. *Nat Commun* **12**, 4474

25. Ma, J., Zheng, B., Goswami, S., Meng, L., Zhang, D., Cao, C., Li, T., Zhu, F., Ma, L., Zhang, Z., Zhang, S., Duan, M., Chen, Q., Gao, Q., and Zhang, X. (2019) PD1(Hi) CD8(+) T cells correlate with exhausted signature and poor clinical outcome in hepatocellular carcinoma. *J Immunother Cancer* **7**, 331

26. Collier, J. L., Weiss, S. A., Pauken, K. E., Sen, D. R., and Sharpe, A. H. (2021) Not-so-opposite ends of the spectrum: CD8(+) T cell dysfunction across chronic infection, cancer and autoimmunity. *Nat Immunol* **22**, 809-819

FIGURE LEGENDS

Figure 1. Increased infiltration of $\alpha_4\beta_7$+ CD3 T cells in the livers of people with NASH and ASH associated cirrhosis. (**A-D**) Serum AST, ALT, bilirubin and gamma-glutamyl transferase (GGT) levels in people without liver disease (disease controls) and people with nonalcoholic steatohepatitis (NASH) and alcoholic steatohepatitis (ASH)-associated cirrhosis. Representative photomicrographs of (**E**) Sirius Red-stained liver biopsies and (**F**) representative confocal images of CD3 (red) and α4β7 (green) immunofluorescence in the liver biopsies. Insets show zoomed-in view of the region in white dotted box. White arrowheads, CD3 T cells. Yellow arrowheads, $\alpha_4\beta_7$+ CD3 T cells. Nuclei are stained blue. Scale bar 100 μm. Data are presented as mean ± SEM. Asterisks indicate significant differences ($p < 0.05$) between disease controls and NASH-associated or ASH-associated cirrhosis.

Figure 2. Integrin $\alpha_4\beta_7$ blockade attenuates CCl_4-induced hepatic inflammation. (**A**) Schematic of study design. Liver fibrosis was induced by oral administration of CCl_4 for six weeks. Mice treated with CCl_4 for six weeks received $\alpha_4\beta_7$ mAb or IgG isotype antibody for four weeks starting at week three. Mice administered the vehicle, olive oil, served as controls (n = 5 - 8 mice per group). (**B**) Representative photomicrographs of Hematoxylin and Eosin (H&E) stained liver tissue sections. (**C-D**) Serum AST and ALT levels. (**E-F**) Expression of key molecules associated with hepatic inflammation (n = 5 - 8 mice per cohort). Data are presented as mean ± SEM. Asterisks indicate significant differences ($p < 0.05$) between oil and IgG isotype

control. Hashtags indicate significant differences ($p < 0.05$) between IgG and $\alpha_4\beta_7$ mAb treatment.

Figure 3. Integrin $\alpha_4\beta_7$ blockade attenuates CCl_4-induced hepatic fibrosis progression. (**A**) Representative photomicrographs of Sirius Red-stained liver tissue sections. Liver fibrosis was induced by oral administration of CCl_4 for six weeks. Mice treated with CCl_4 for six weeks received $\alpha_4\beta_7$ mAb or IgG isotype antibody for four weeks starting at week three. Mice administered the vehicle, olive oil, served as controls (n = 5 - 8 mice per group). (**B-F**) Expression of fibrosis markers in the liver tissue sections. (**G**) Representative confocal images of αSMA (green) immunofluorescence in the liver (n = 5 mice per cohort). Nuclei are stained blue. Scale bar 100 μm. Data are presented as mean ± SEM. Asterisks indicate significant differences ($p < 0.05$) between oil and IgG isotype control. Hashtags indicate significant differences ($p < 0.05$) between IgG and $\alpha_4\beta_7$ mAb treatment.

Figure 4. Integrin $\alpha_4\beta_7$ mAb treatment reduces CCl_4-induced infiltration of $\alpha_4\beta_7$+ T cells in the liver. (**A**) Representative confocal images of $\alpha_4\beta_7$ (red) immunofluorescence in the liver. Mice treated with CCl_4 for six weeks received $\alpha_4\beta_7$ mAb or IgG isotype antibody for four weeks starting at week three. Mice administered the vehicle, olive oil, served as controls (n = 5 - 8 mice per group). Nuclei are stained blue. (**B-D**) Expression of (**B**) integrin α_4, *Itga4*, (**C**) integrin β_7, *Itgb7* and (**D**) integrin β_1, *Itgb1* in the liver (n = 5). (**E-F**) Bar graphs show percentage and total number of (**E**) CD4 and (**F**) CD8 T cells in the liver (n = 5). (**G-H**) Bar graphs show percentage and total number of (**G**) $\alpha_4\beta_7$+ CD4 and (**H**) $\alpha_4\beta_7$+ CD8 T cells in the liver (n = 5). Data are presented as mean ± SEM. Asterisks indicate significant differences ($p < 0.05$) between oil and

IgG isotype control. Hashtags indicate significant differences ($p < 0.05$) between IgG and $\alpha_4\beta_7$ mAb treatment.

Figure.5. MAdCAM-1 blockade reduces CCL_4-induced infiltration of $\alpha_4\beta_7$+ T cells in the liver. (**A-B**) Representative flow plots show percent of $\alpha_4\beta_7$+ CD4 T cells, and bar graphs show percentage and total number of $\alpha_4\beta_7$+ CD4 T cells in the liver. Mice treated with CCl_4 for six weeks received MAdCAM-1 mAb or IgG isotype antibody for four weeks starting at week three (n = 5 - 8 mice per cohort). (**C-D**) Representative flow plots show percent of $\alpha_4\beta_7$+ CD8 T cells, and bar graphs show percentage and total number of $\alpha_4\beta_7$+ CD8 T cells in the liver. (**E-F**) Percentage and total number of macrophages (CD3-CD11b+Ly6G-F4/80+ cells) and monocytes (CD3-CD11b+Ly6G-Ly6C+ cells) in the liver. (**G-I**) Expression of (**G**) integrin α_4, *Itga4*, (**H**) integrin β_7, *Itga7* and (**I**) *Madcam-1* in the liver (n = 5). Data are presented as mean ± SEM. Hashtags indicate significant differences ($p < 0.05$) between IgG and MAdCAM-1 mAb treatments.

Figure.6. $\alpha_4\beta_7$+ CD4 T cells enriched for markers of activation and proliferation demonstrating an effector phenotype. (**A**) Representative histograms show median fluorescence intensity of stated markers in the liver of mice treated with CCl_4 for six weeks. Mice were treated with IgG during the final four weeks (n = 5). Bar graphs show percentage of $\alpha_4\beta_7$+ and $\alpha_4\beta_7$- CD4 T cells expressing T cell activation markers (**B**) CD44 and CD69, (**C**) Th1 cell marker Tbet and (**D**) proliferation marker Ki67 in the liver (n = 5).

Figure. 7. MAdCAM-1 blockade attenuates hepatic inflammation and fibrosis progression. (**A**) Representative photomicrographs of Hematoxylin and Eosin (H&E) stained liver tissue sections. Mice treated with CCl_4 for six weeks received MAdCAM-1 mAb or IgG isotype antibody for four weeks starting at week three (n = 5 - 8 mice per group). (**B**) Serum ALT level. (**C-E**) Expression of key molecules associated with hepatic inflammation (n = 5- 8 mice per group). (**F**) Representative photomicrographs of Sirius Red-stained liver tissue sections. (**G-J**) Expression of key fibrosis markers in the liver. Data are presented as mean ± SEM. Hashtags indicate significant differences ($p < 0.05$) between IgG and MAdCAM-1 mAb treatments.

FIGURES

Figure 1

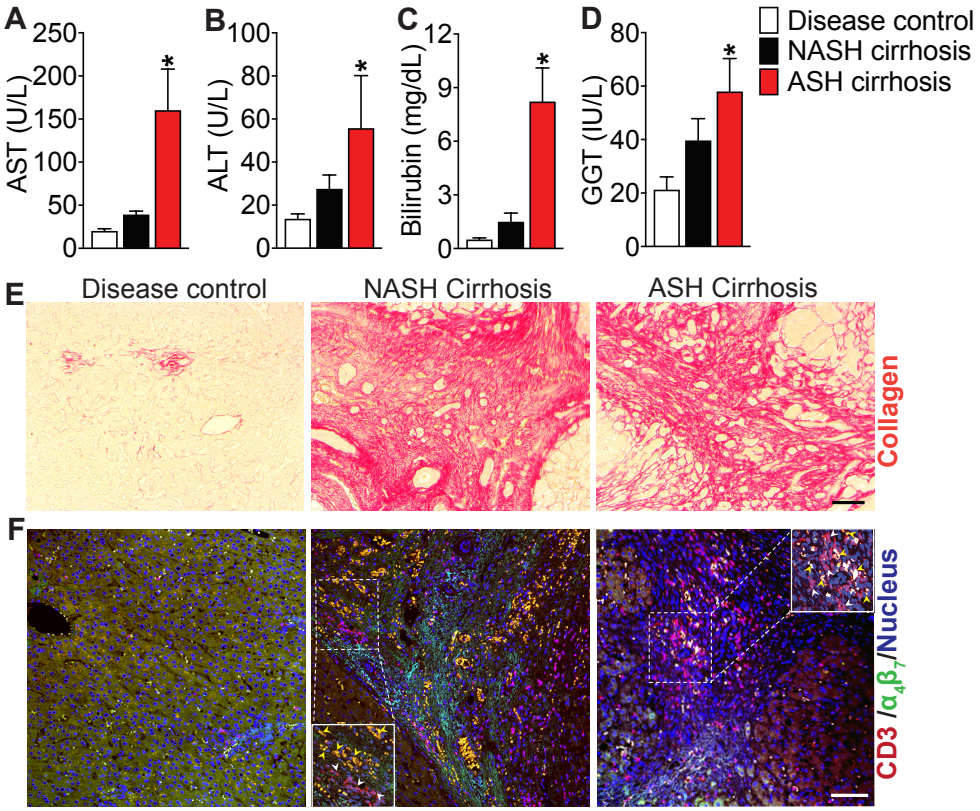

Figure 2

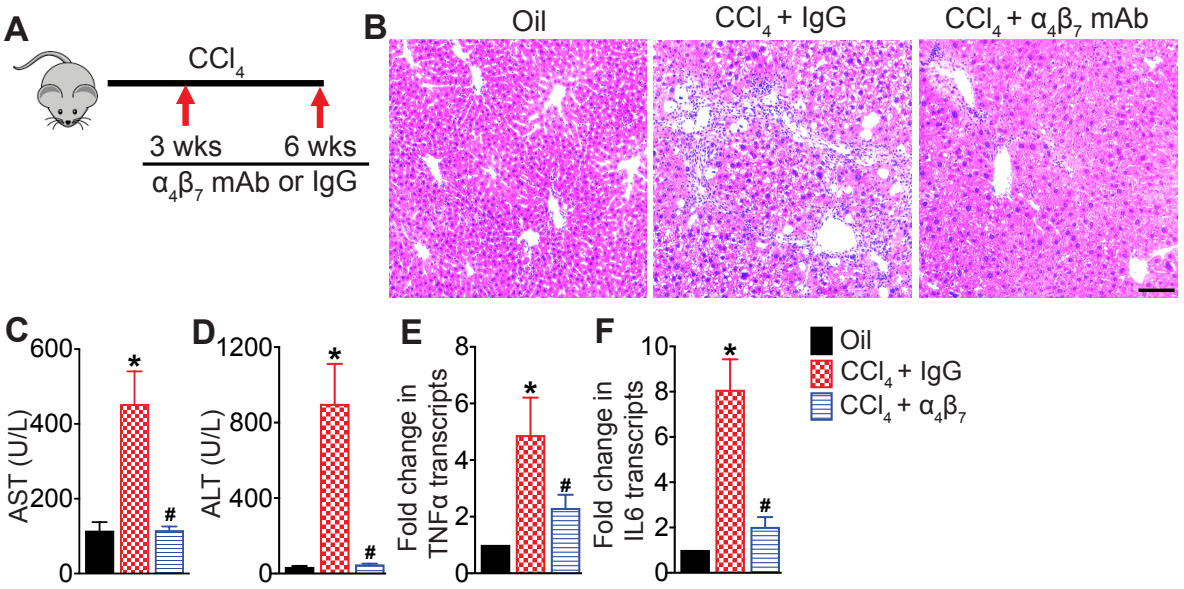
A
CCl4
3 wks
6 wks
α4β7 mAb or IgG
B
Oil
CCl4 + IgG
CCl4 + α4β7 mAb
C
AST (U/L)
600
400
200
0
D
ALT (U/L)
1200
800
400
0
E
Fold change in TNFα transcripts
8
6
4
2
0
F
Fold change in IL6 transcripts
10
8
6
4
2
0
*
#
Oil
CCl4 + IgG
CCl4 + α4β7

Figure 3

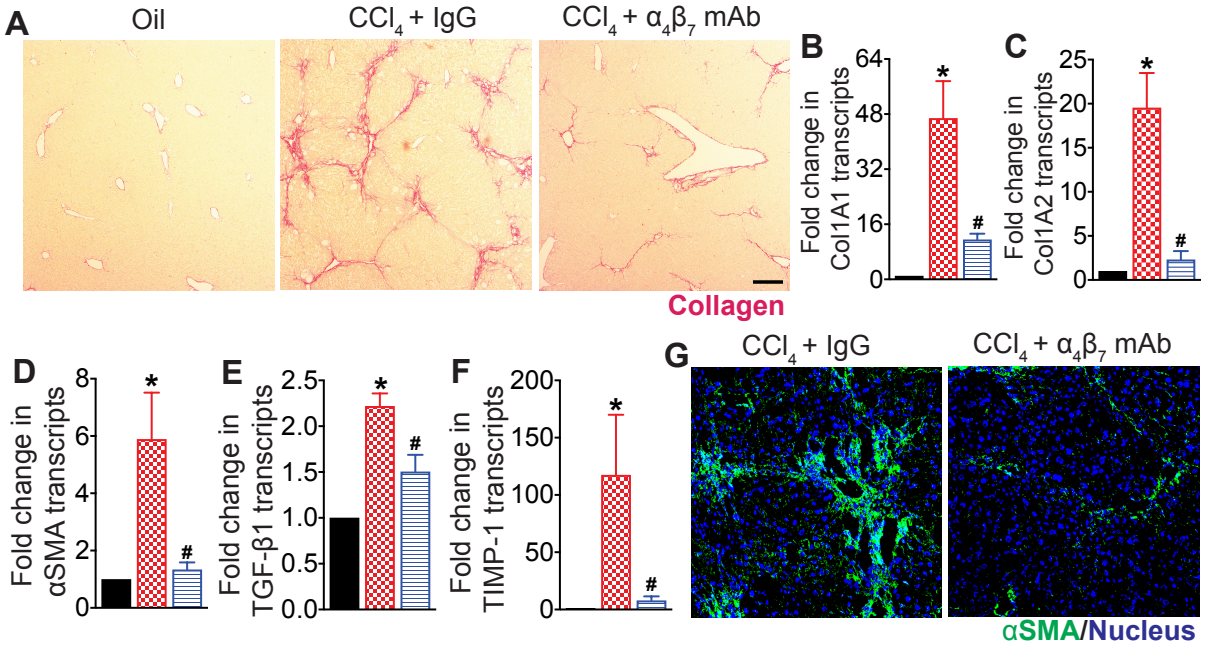
A
Oil
CCl4 + IgG
CCl4 + α4β7 mAb
Collagen
B
Fold change in Col1A1 transcripts
64
48
32
16
0
*
#
C
Fold change in Col1A2 transcripts
25
20
15
10
5
0
*
#
D
Fold change in αSMA transcripts
8
6
4
2
0
*
#
E
Fold change in TGF-β1 transcripts
2.5
2.0
1.5
1.0
0.5
0.0
*
#
F
Fold change in TIMP-1 transcripts
200
150
100
50
0
*
#
G
CCl4 + IgG
CCl4 + α4β7 mAb
αSMA/Nucleus

Figure 4

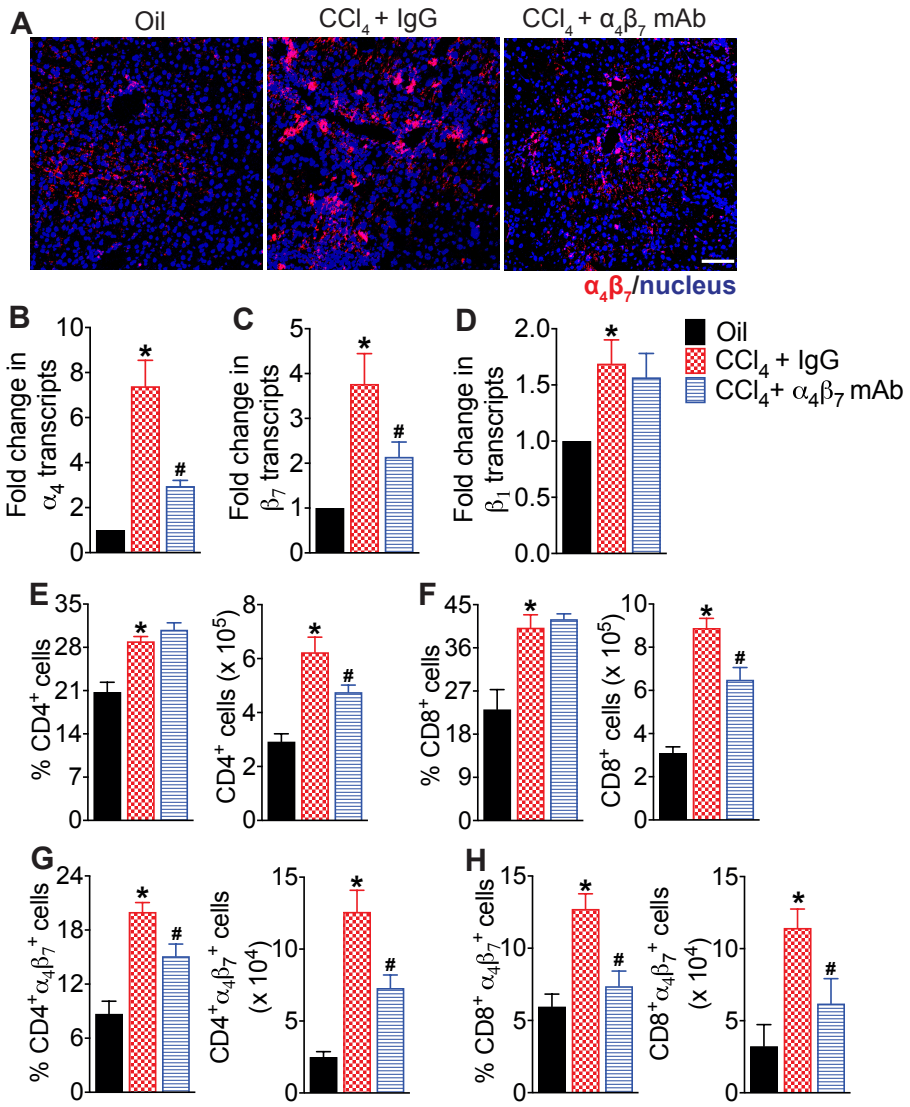
A
Oil
CCl4 + IgG
CCl4 + α4β7 mAb
α4β7/nucleus
B
Fold change in α4 transcripts
C
Fold change in β7 transcripts
D
Fold change in β1 transcripts
Oil
CCl4 + IgG
CCl4+ α4β7 mAb
E
% CD4+ cells
CD4+ cells (x 10^5)
F
% CD8+ cells
CD8+ cells (x 10^5)
G
% CD4+α4β7+ cells
CD4+α4β7+ cells (x 10^4)
H
% CD8+ α4β7+ cells
CD8+α4β7+ cells (x 10^4)

Figure 5

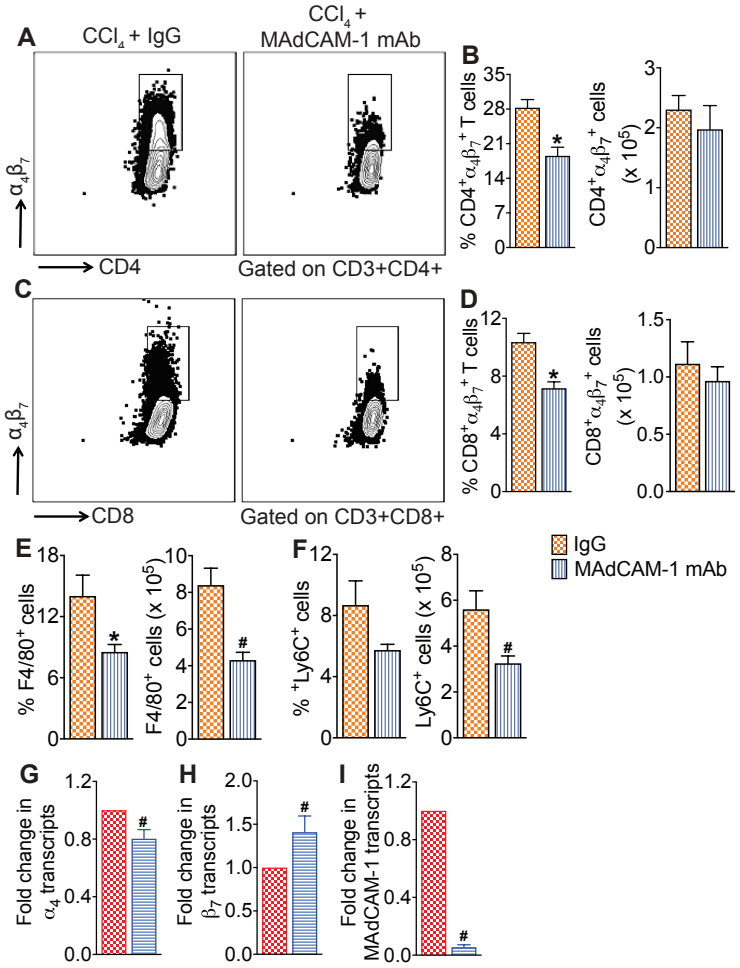
A
CCl4 + IgG
CCl4 + MAdCAM-1 mAb
α4β7
CD4
Gated on CD3+CD4+
B
% CD4+α4β7+ T cells
CD4+α4β7+ cells (x 10^5)
C
CD8
Gated on CD3+CD8+
D
% CD8+α4β7+ T cells
CD8+α4β7+ cells (x 10^5)
IgG
MAdCAM-1 mAb
E
% F4/80+ cells
F4/80+ cells (x 10^5)
F
% +Ly6C+ cells
Ly6C+ cells (x 10^5)
G
Fold change in α4 transcripts
H
Fold change in β7 transcripts
I
Fold change in MAdCAM-1 transcripts

Figure 6

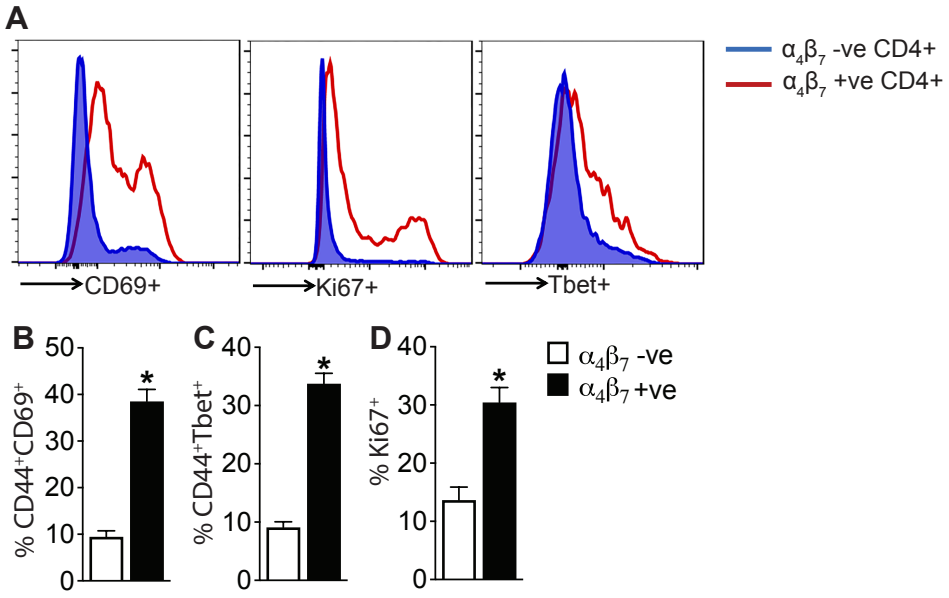
A
α4β7 -ve CD4+
α4β7 +ve CD4+
CD69+
Ki67+
Tbet+
B
% CD44+CD69+
50
40
30
20
10
0
*
C
% CD44+Tbet+
40
30
20
10
0
*
D
% Ki67+
40
30
20
10
0
*
α4β7 -ve
α4β7 +ve

Figure 7

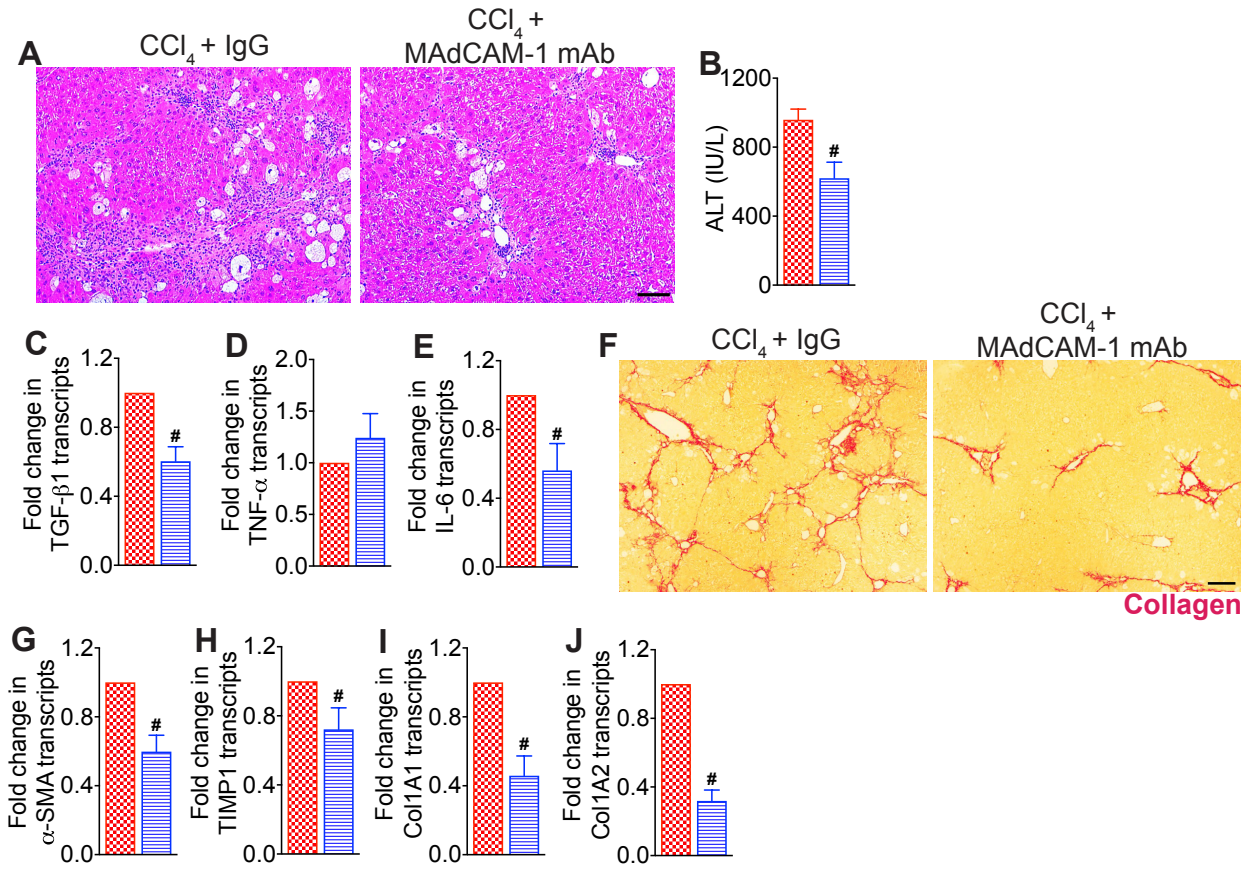
A
CCl4 + IgG
CCl4 +
MAdCAM-1 mAb
B
ALT (IU/L)
1200
800
400
0
#
C
Fold change in
TGF-β1 transcripts
1.2
0.8
0.4
0.0
#
D
Fold change in
TNF-α transcripts
2.0
1.5
1.0
0.5
0.0
E
Fold change in
IL-6 transcripts
1.2
0.8
0.4
0.0
#
F
CCl4 + IgG
CCl4 +
MAdCAM-1 mAb
Collagen
G
Fold change in
α-SMA transcripts
1.2
0.8
0.4
0.0
#
H
Fold change in
TIMP1 transcripts
1.2
0.8
0.4
0.0
#
I
Fold change in
Col1A1 transcripts
1.2
0.8
0.4
0.0
#
J
Fold change in
Col1A2 transcripts
1.2
0.8
0.4
0.0
#